Journal of Molecular Catalysis A: Chemical 287 (2008) 45–52

Contents lists available at ScienceDirect

Journal of Molecular Catalysis A: Chemical

journal homepage: www.elsevier.com/locate/molcata

Ziegler-Natta catalysts for propylene polymerization: Chemistry of reactions leading to the formation of active centers

Yury V. Kissin[a,*], Xinsheng Liu[b], David J. Pollick[b], Nancy L. Brungard[b], Main Chang[c]

[a] Rutgers, The State University of New Jersey, Department of Chemistry and Chemical Biology, 610 Taylor Road, Piscataway, NJ 08854, USA
[b] BASF, Research Center, 101 Wood Avenue, Iselin, NJ 08830, USA
[c] BASF, 10001 Chemical Road, Pasadena, TX 77507, USA

ARTICLE INFO

Article history:
Received 14 December 2007
Accepted 27 February 2008
Available online 6 March 2008

Keywords:
Ziegler-Natta catalyst
Infrared spectroscopy, of Ziegler-Natta catalysts
NMR spectroscopy, of Ziegler-Natta catalysts

ABSTRACT

The article describes chemical reactions between a fourth-generation solid Ziegler-Natta catalyst for propylene polymerization, $TiCl_4/MgCl_2$/diisobutyl phthalate (DIBP), and cocatalyst mixtures containing $AlEt_3$ and an external donor compound, $(Cy)(Me)Si(OMe)_2$. The solid catalyst component contains several surface complexes of diisobutyl phthalate with $MgCl_2$ and $TiCl_4$, as well as complexes of $MgCl_2$ and *o*-phthaloyl chloride, which is formed in a reaction between DIBP and $TiCl_4$. When the solid catalyst is contacted with the cocatalyst mixture, all these adsorbed carbonyl species react with $AlEt_3$. The reactions reduce the carbonyl groups of DIBP and lead to the formation of various dialkylaluminum alkoxides. The order of reactivity of the complexes in the reactions with $AlEt_3$ is: phthaloyl chloride/$MgCl_2$ > DIBP/$MgCl_2$ ≈ DIBP/$TiCl_4$. These reactions result in a complete removal of phthaloyl chloride from the catalyst surface, in a significant reduction of the total content of the $MgCl_2$/DIBP and $TiCl_4$/DIBP complexes, and in the reduction of surface Ti^{IV} species to Ti^{III}. The second component of the cocatalyst mixture, complexes of $(Cy)(Me)Si(OMe)_2$ with $AlEt_3$, are strongly adsorbed on the surface of the solid catalyst and on the surface of the products of its reactions with excess $AlEt_3$. The most probable coordination site for the silane species is surface Ti atoms, including the active centers in olefin polymerization reactions.

1. Introduction

Supported Ziegler-Natta catalysts for olefin polymerization represent an example of catalysts which, formally heterogeneous, exhibit all the features typical for molecular catalysis: initial chemical species in them are known, and chemical reactions leading to the formation of active centers are a subject of the arsenal of analytical methods common for the latter type of catalysis, NMR, IR, etc. This paper describes chemical reactions leading to the formation of active centers in a fourth-generation supported $TiCl_4/MgCl_2$ catalyst designed for isospecific polymerization of propylene and other α-olefins.

The catalysts of the fourth-generation contain alkyl esters of aromatic *ortho*-diacids (internal donor compounds) as components of the solid catalysts and alkoxysilanes (external donor compounds) as components of cocatalyst mixtures. In general, these catalysts employ highly porous spherical particles of anhydrous $MgCl_2$ as a support/carrier. Several techniques were developed for the manufacture of $MgCl_2$ particles suitable for the catalyst preparation [1]. They include: (a) crystallization of molten $MgCl_2$/alcohol complexes in inert dispersants at low temperature [2]; (b) precipitation of $MgCl_2$ complexes with alcohols or other polar compounds from solution followed by their thermal or chemical decomposition with the formation of microcrystalline $MgCl_2$ [2,3]; and (c) synthesis of $MgCl_2$ from alkylmagnesium compounds, by reacting them with chloro-containing reagents such as HCl, RCl, $SiCl_4$, $TiCl_4$, etc. [4]. After the $MgCl_2$ particles are formed, esters of aromatic *ortho*-diacids and $TiCl_4$ are deposited on their surface.

These catalysts are activated in polymerization reactions with combinations of $AlEt_3$ and alkylalkoxy or arylalkoxysilanes, $R_xSi(OR')_{4-x}$. The molar [Al]:[Si] ratio in the cocatalyst mixtures varies from 10:1 to 20:1, and the molar [Al]:[Ti] ratio in the final catalyst systems is ~250 [5–10]. One group of such solid catalysts is manufactured by BASF. Their productivity exceeds 50 kg of polypropylene per gram of catalyst, and the yield of the crystalline isotactic fraction in the polymers they produce ranges from 97 to 99%, depending on the type and the amount of an added silane compound.

A number of publications describe chemical and spectroscopic analysis of various solid components of these catalyst systems, as

* Corresponding author. Tel.: +1 732 445 5882.
E-mail address: ykissin@rci.rutgers.edu (Y.V. Kissin).

1381-1169/$ – see front matter © 2008 Elsevier B.V. All rights reserved.
doi:10.1016/j.molcata.2008.02.026

well as the structures of various model systems [10–14]. The present paper is mostly devoted to the analysis of one final catalyst system, the product of the interaction between the solid catalyst and the solution of the cocatalyst mixture. These reactions lead to the formation of active centers in olefin polymerization reactions.

2. Experimental

2.1. Solid catalyst

The catalyst was synthesized according to the earlier described procedure [15–17]. The support was $MgCl_2$ in a microcrystalline form [16]. The particular example of the catalyst used diisobutyl phthalate (DIBP) as a model internal electron donor at a molar [DIBP]:[Mg] ratio of 0.25. The final composition of the solid is: [Ti] ~1.9 wt.%, [Mg] ~18 wt.%, [Cl] ~56 wt.%, [phthalate] ~13 wt.% [17]. In general terms, the catalyst can be viewed as microcrystalline $MgCl_2$ containing Ti species at [Ti]:[Mg] = 0.055 and different phthalate-derived species on the surface of $MgCl_2$ crystals [16].

The earlier microscopic and XRD analysis of the catalyst [16] showed that its primary particles are spherical, 5–10 μm in diameter, and consist of radically spreading, relatively narrow (500–1000 Å) and relatively long (≤500 nm) rod-like structures built of very small crystallites of $MgCl_2$ ~30–40 Å in size.

2.2. Chemical reactions

This solid catalyst was contacted with cocatalysts, mixtures of $AlEt_3$ and cyclohexyl,methyl dimethoxysilane, (Cy)(Me)Si(OMe)$_2$. These reactions were carried out under nitrogen in 10-cc and 20-cc glass vials capped with rubber septa. Table 1 gives the reaction conditions. In order to observe transformations of DIBP in the catalyst systems, experiments 1 and 2 were carried out at low [Al]:[Ti] ratios, which translate into very low [Al]:[phthalate] ratios. Experiments 3–5 were carried out at high [Al]:[Ti] ratios, which are similar to the ratios typically encountered in propylene polymerization reactions, although the $AlEt_3$ concentration in these experiments, 1 M, was much higher than in real polymerization reactions.

A number of additional model experiments were carried out. Their conditions are given in Table 2. Complexes of anhydrous $MgCl_2$ with DIBP, ethyl benzoate, and *o*-phthaloyl chloride were prepared by dispersing $MgCl_2$ crystals in solutions of the carbonyl-containing compounds in *n*-heptane at 20 °C under nitrogen using a high-speed stirring devise (Tearor) rotating at 35,000 rpm. Solid materials in the mixtures were separated and thoroughly washed with heptane.

2.3. Spectroscopic methods

IR spectroscopic studies were carried out on a Bio-Rad FTS 6000 FT-IR spectrometer. Two types of spectra were recorded, transmittance spectra using slurries in dry inert media, Nujol and Fluorolube, and diffuse reflectance spectra, using a SpectraTec diffuse reflectance attachment. All IR samples were prepared in a nitrogen glove box. The sample cavity in the diffuse reflectance attachment was sealed inside the glove box to prevent exposure of the catalyst samples to atmosphere.

^{1}H, ^{13}C, ^{29}Si, and ^{27}Al NMR spectra of soluble reaction products were recorded on a Varian Mercury 300 NMR spectrometer and a Varian Unity Inova 400 NMR spectrometer at 25 °C at the spinning rate of 20 Hz. Deuterated chloroform in sealed glass inserts was used as a reference and a lock solvent.

XPS spectra were recorded with a VG 220i XL photoelectron spectrometer; standard charge compensation protocols were used to eliminate charging effects. A pass resolution of 20 eV and a spot size of 500 μm were used.

Diffuse reflectance UV–vis spectra were recorded on a Varian 300 spectrophotometer equipped with an integrating sphere. Packed Teflon power in an aluminum holder was used as a background. A quartz tube cell was used for the measurements with the same background Teflon powder.

Table 1
Conditions of reactions between solid catalyst, $AlEt_3$, and (Cy)(Me)Si(OMe)$_2$, reaction time 20 min

Experiment	[Al]:[Ti]	[Al]:[(C=O)]	[Si]:[Al]	Temperature (°C)
1	24	2.4	1:10	20
2	30	2.8	1:11	70
3	184	19	1:10	80
4	180	18	1:10	80
5	173	18	1:10	80
cocatalyst mixture was not washed out				
6	240	24	0	80

Table 2
Reaction conditions for model mixtures

Experiment	Composition of mixture	Temperature (°C)	Time (min)
$AlEt_3$ + (Cy)(Me)Si(OMe)$_2$			
7	[Al]:[Si] = 8.3	20	60
8	[Al]:[Si] = 8.3	70	30
$AlEt_3$ + DIBP			
9	[Al]:[DIBP] = 10.5	20	15 and 500
10	[Al]:[DIBP] = 10.5	70	30
$MgCl_2$ + (Cy)(Me)Si(OMe)$_2$			
11	[Mg]:[Si] = 23	20	10
Solid catalyst + (Cy)(Me)Si(OMe)$_2$			
12	[Mg]:[Si] = 8.1	20	30
$MgCl_2$ + DIBP			
13	[Mg]:[DIBP]~5	20	10
14–19	[Mg]:[DIBP] 0.6–7	20	1
$MgCl_2$ + EB			
20–24	[Mg]:[EB] 0.45 to ~8	20	1
$MgCl_2$ + PHTHCl			
25, 26	[Mg]:[PHTHCl] 1, 2	20	1

3. Results and discussion

Before the reaction products between the solid catalyst and the cocatalyst mixtures are determined, the chemical compounds present in each reaction component, the catalyst and the cocatalyst, have to be examined. Therefore, the experimental data below are divided into three sections describing the chemical structures of the solid catalyst, the cocatalyst, and, finally, the chemistry of their interactions.

3.1. Solid catalyst: identification of carbonyl species

It is generally assumed that the internal electron donors in the Ziegler-Natta catalysts of the fourth-generation are aliphatic esters of *ortho*-aromatic diacids (DIBP in this study), the same compounds that are used in the synthesis of the solid catalysts. IR spectroscopy is the preferred technique for their analysis. Fig. 1 gives the IR spectrum of the solid catalyst in the 1900–1550 cm^{-1} spectral range. It contains a complex envelope of ν(C=O) bands as well as two narrow bands of the *ortho*-disubstituted benzene ring of DIBP at 1595 and 1582 cm^{-1}. The literature [10–12,14] assigns the ν(C=O) bands to several types of complexes: complexes of DIBP with

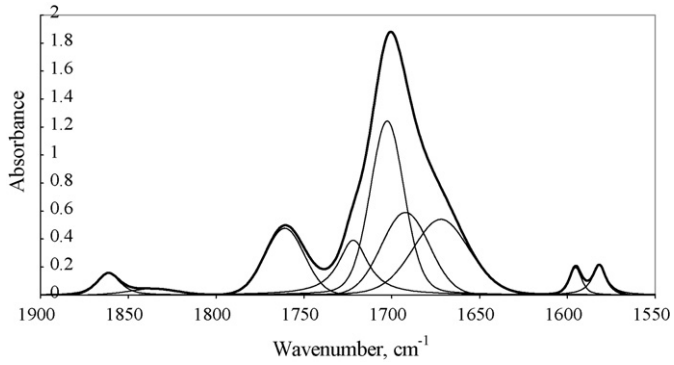

Fig. 1. Transmission IR spectrum of solid catalyst, the ν(C=O) range.

$MgCl_2$ and $TiCl_4$, and complexes of $MgCl_2$ with two derivatives of DIBP, phthaloyl chloride (PHTHCl), and *o*-phthaloyl monochloride, C_6H_4(COCl)(COO*i*-Bu). The last two compounds are the expected products of reactions between DIBP and $TiCl_4$, which take place in the course of the catalyst synthesis at high temperatures:

$$C_6H_4[C(=O)\text{–}O\text{-}i\text{–}Bu]_2 + TiCl_4 \rightarrow C_6H_4[C(=O)\text{–}Cl][C(=O)\text{–}O\text{–}i\text{-}Bu] + Ti(Oi\text{-}Bu)Cl_3 \quad (1)$$

$$C_6H_4[C(=O)\text{–}Cl][C(=O)\text{–}O\text{–}i\text{-}Bu] + TiCl_4 \rightarrow C_6H_4[C(=O)\text{–}Cl]_2 + Ti(Oi\text{-}Bu)Cl_3 \quad (2)$$

We re-examined the chemical composition of carbonyl complexes in the solid catalyst by separately preparing complexes of $MgCl_2$ with two of the expected carbonyl-containing compounds, DIBP and PHTHCl, as well as model complexes of $MgCl_2$ and the external donor in the catalysts of the third-generation, ethyl benzoate (EB). These data, as well as the published IR spectroscopic information [10–12,14] provided the basis for IR band assignment.

3.1.1. Model mixtures: ester/$MgCl_2$ and PHTHCl/$MgCl_2$ complexes

Mixtures of anhydrous $MgCl_2$ with DIBP were vigorously agitated at 20 °C (Table 2) and IR spectra of their solid components were recorded. All these spectra are overlaps of the IR spectrum of free DIBP physisorbed on the $MgCl_2$ surface [a single symmetric ν(C=O) band at 1733 cm^{-1}] and the spectra of its complexes with $MgCl_2$. The latter are shown in Fig. 2. The $MgCl_2$/DIBP complexes

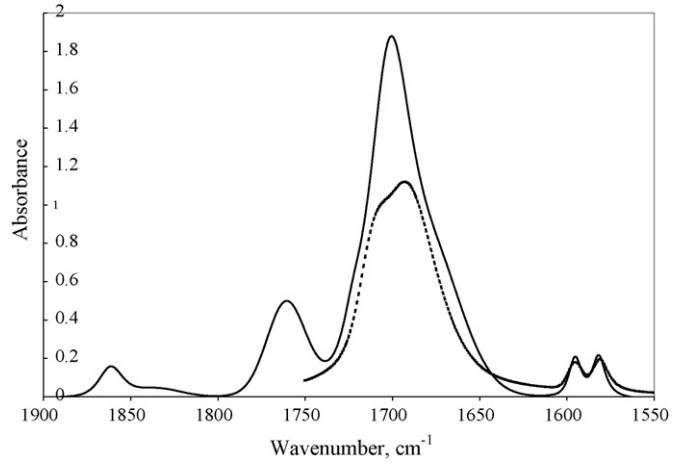

Fig. 2. Comparison of two spectra in the ν(C=O) range: catalyst (solid line) and $MgCl_2$/DIBP complexes (dotted line). The spectrum of the complexes was produced by subtracting the spectrum of free DIBP from the spectra of $MgCl_2$–DIBP mixtures.

Table 3
Complexes in DIBP–$MgCl_2$ mixtures, IR data

[DIBP]:[$MgCl_2$] (mmol/g)	Fraction of DIBP in complexes (%)
0.14	91
0.19	64
0.42	80
0.43	55
0.98	68
1.63	28

produce an asymmetric envelope of ν(C=O) bands at ~1695 cm^{-1}. Spectral resolution shows that two complexes of a similar strength are represent, their IR bands are at ~1710 and 1692 cm^{-1}. The fraction of DIBP in the complexes decreases with an increase of the [DIBP]:[$MgCl_2$] ratio in DIBP–$MgCl_2$ mixtures (Table 3). An approximate estimation shows that only 0.07–0.1 mmol of DIBP is present on the $MgCl_2$ surface in the form of the complexes at this level of $MgCl_2$ dispersion. EB in EB–$MgCl_2$ mixtures (Table 2) forms complexes of a similar type; their ν(C=O) bands are at ~1700–1695, ~1685, and ~1665 cm^{-1}. The similarity between the $\Delta\nu$(C=O) values for the $MgCl_2$ complexes with EB (which can only be a monodentate ligand) and the $MgCl_2$ complexes with DIBP suggests that each carbonyl group in the latter complexes is also most probably a monodentate ligand coordinated to a single Mg^{2+} ion. For example, each of the two carbonyl groups in the DIBP molecule can be coordinated either to neighboring Mg^{2+} cations on the (1 1 0) face or on the (1 0 0) face of $MgCl_2$ crystallites. Another possible coordination type of a DIBP molecule, as a bidentate ligand to a single Mg^{2+} ion, is less probable, although the presence of such complexes in the $MgCl_2$–DIBP mixtures [their ν(C=O) band is expected at ~1720 cm^{-1}] cannot be excluded.

Because PHTHCl can be formed in the course of the catalyst synthesis (reaction (2)) [12], its complexes with $MgCl_2$ were also prepared. The IR spectrum of neat PHTHCl in the ν(C=O) range is very complex; it contains nine bands: three small, at 1857, 1845, and 1815 cm^{-1}, two dominant, at 1801 and 1792 cm^{-1}, and four weaker bands at 1777, 1758, 1741, and 1715 cm^{-1}. IR spectra of the solid products formed in vigorously agitated PHTHCl–$MgCl_2$ mixtures at [PHTHCl]:[$MgCl_2$] ratios of ~0.5 and ~1 (Table 2) contain three overlapping groups of bands, those of free PHTHCl, physisorbed PHTHCl (at ~1860, ~1850, and ~1825 cm^{-1}), and PHTHCl/$MgCl_2$ complexes themselves. The main ν(C=O) bands in the latter are at 1766 cm^{-1} (the dominant band), 1734 and 1694 cm^{-1}. The $\Delta\nu$(C=O) value for the main band of the complexes vs. that of the free PHTHCl is in the range of 25–35 cm^{-1}, a relatively small value indicating that the C(Cl)=O···Mg^{2+} coordination in the complexes is weak.

3.1.2. Carbonyl-containing species in the solid catalyst

Fig. 1 shows resolution of the ν(C=O) envelope in the IR spectrum of the solid catalyst assuming the mixed Lorentz/Gaussian shape of individual bands. The band assignment is based on three sets of data: (a) the literature [10,12,14], (b) the above-described IR data for surface complexes of $MgCl_2$ with DIBP, EB, and PHTHCl, and (c) the effects of the catalyst treatment with $AlEt_3$ on the relative absorbance of different bands (described in Section 3.3).

Several types of carbonyl species are present in the solid catalyst. The species of the first type are complexes of DIBP and $MgCl_2$. In the literature [10,12,14], a group of medium-broad overlapping bands with the maximum at 1720–1670 cm^{-1} is assigned to these complexes. The IR band resolution suggests the existence of three such species with the bands at ~1700 and 1692 cm^{-1} and a shoulder at ~1720 cm^{-1}. The difference between the positions of the two largest ν(C=O) bands, ~10 cm^{-1}, indicates that the two major DIBP/$MgCl_2$ complexes are quite similar. Fig. 2 compares the spectra of the solid catalyst and that of the DIBP/$MgCl_2$ complexes in

the ν(C=O) range. The positions of the ν(C=O) bands in the spectra of the DIBP–$MgCl_2$ mixtures are very close to their positions in the catalyst spectrum. Because the IR spectra of EB/$MgCl_2$ complexes (described above) also have the ν(C=O) bands at practically the same wavenumbers, the similarity suggests that all DIBP/$MgCl_2$ complexes in the catalyst have a similar chemical nature with DIBP molecules as monodentate ligands, whereas the small band at ~1720 cm^{-1} (see Fig. 1) can be due to a bidentate DIBP/$MgCl_2$ complex.

The second group of identifiable species in the catalyst belong to PHTHCl: the bands at 1861, ~1835, and 1761 cm^{-1}. The medium–strong band at 1761 cm^{-} clearly belongs to the PHTHCl/$MgCl_2$ complex and two bands at 1861 and ~1835 cm^{-1} to PHTHCl physically adsorbed on the $MgCl_2$ surface. The extent of reaction (2) during the catalyst synthesis is quite significant. If one assumes that the integral absorbance coefficients for all ν(C=O) bands are similar, 15–20% of DIBP is converted to PHTHCl. Over 70% of the produced PHTHCl forms complexes with $MgCl_2$. In the literature [12], the shoulder at 1720 cm^{-1} in the spectrum of a similar catalyst is assigned to a complex of $MgCl_2$ with *o*-phthaloyl monochloride formed in reaction (1). However, the IR spectrum of the DIBP/$MgCl_2$ complex also contains a strong shoulder at 1720–1710 cm^{-1} (Fig. 2), and the assignment of the 1720 cm^{-1} band in the spectrum of the catalyst (Fig. 1) to a DIBP/$MgCl_2$ complex appears more reasonable.

The third type of carbonyl species in the catalyst is the complex of DIBP and $TiCl_4$. Complexes of $TiCl_4$ and esters of aromatic acids are thoroughly described in the literature [12,13,18–20]. Two types of such complexes exist in which the esters act as monodentate or bidentate ligands. Esters of benzoic acid form strong monodentate complexes with $TiCl_4$ [18–20]; the $\Delta\nu$(C=O) value for them ranges from 135 to 145 cm^{-1}. Diesters of phthalic acid form 1:1 complexes with $TiCl_4$ in which the diesters act as bidentate ligands: both of their carbonyl groups are coordinated to the same Ti atom [12]. The ν(C=O) bands in the IR spectra of the latter complexes are at ~1650 cm^{-1}, i.e., the $\Delta\nu$(C=O) values are much lower, ~75–80 cm^{-1}. The complex of DIBP and $TiCl_4$ in the catalyst has a broad IR band at ~1670 cm^{-1}; its low $\Delta\nu$(C=O) value suggests that DIBP forms a bidentate complex with $TiCl_4$. The high width of the band (see Fig. 1) indicates that it is probably an overlap of two closely positioned bands of different $TiCl_4$ complexes. The content of DIBP in its complexes with $TiCl_4$ accounts for ~20% of all DIBP molecules in the catalyst.

The investigated catalyst, as all Ziegler-Natta catalysts, is very sensitive to moisture. Even a brief, 1–2 s, exposure of the catalyst to air results in a noticeable spectral change: two broad bands appear at ~1655 and ~1620 cm^{-1}. The same bands are present in the spectra of the solid catalyst treated with $AlEt_3$ and briefly exposed to air. The most probable assignment of these two bands is the $\nu(H_2O)$ mode in $MgCl_2$ hydrates. The attribution of these bands to very strong complexes between the diesters and $MgCl_2$ proposed in the literature [14] does not agree with their absence in DIBP–$MgCl_2$ mixtures (Fig. 2).

3.2. Composition of cocatalyst mixtures

Reactions between organoaluminum catalysts and silyl ethers $R_nSi(OMe)_{4-n}$ were studied earlier by ^{13}C NMR and IR [26]. Our NMR data mostly agree with the literature. Fig. 3 shows ^1H spectra of (Cy)(Me)$Si(OMe)_2$ and the early products of its reaction with $AlEt_3$ at 20 °C (Table 2, experiment 7). Several complexes are rapidly formed in the mixture of $AlEt_3$ and (Cy)(Me)$Si(OMe)_2$ at [Al]:[Si] ~8. The complexes are strongly asymmetrical and exhibit several characteristic features:

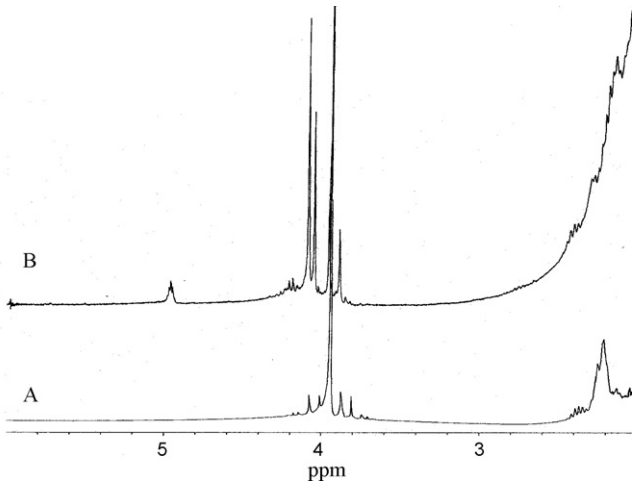

Fig. 3. ^1H NMR spectra of (CH)(Me)$Si(OMe)_2$ (A) and the early products formed in (Cy)(Me)$Si(OMe)_2$–$AlEt_3$ mixture at 70 °C ((B) Table 2, experiment 7).

1. Four CH_3–(O–Si) signals at 3.89, 3.96, 4.05, and 4.09 ppm in the ^1H NMR spectrum vs. 3.92 ppm for pure (Cy)(Me)$Si(OMe)_2$ (Fig. 3).
2. CH_3–(O–Si) signals at 50.6, 53.6, and 55.5 ppm and the CH_3–(Si) signal at −5.8 ppm in the ^{13}C NMR spectrum vs. 49.7 and −8.2 ppm for (Cy)(Me)$Si(OMe)_2$, respectively.

Judging by the low intensity of the 49.7 ppm signal of free (Cy)(Me)$Si(OMe)_2$ in the ^{13}C NMR spectrum, ~70–80% of the silane molecules in this mixture form complexes with $AlEt_3$.

These (Cy)(Me)$Si(OMe)_2$/$AlEt_3$ complexes are not stable. As was first noticed in Ref. [26], an exchange reaction takes place over time, especially at elevated temperatures (Table 2, experiment 8):

$$AlEt_3 + (Cy)(Me)Si(OMe)_2 \rightarrow AlEt_2(OMe) + (Cy)(Me)(Et)Si(OMe) \quad (3)$$

This reaction is relatively slow and never comes to completion. The silane molecule produced in reaction (3), (Cy)(Me)(Et)Si(OMe), also forms complexes with excess of $AlEt_3$.

Reaction (3) results in a number of changes in NMR spectra. A complex CH_3–(Si) signal pattern develops in the ^1H NMR spectrum: a new series of weak signals of the (Cy)(Me)(Et)Si(OMe)/$AlEt_3$ complexes appears in the 0.40–0.52 ppm range in addition to the signals of the original (Cy)(Me)$Si(OMe)_2$/$AlEt_3$ complexes at 0.30, 0.33 and 0.36 ppm. The (Cy)(Me)(Et)Si(OMe)/$AlEt_3$ complexes also give rise to a new CH_3–(O–Si) signal at 55.6 ppm in the ^{13}C NMR spectrum whereas ^{13}C NMR signals of the original (Cy)(Me)$Si(OMe)_2$/$AlEt_3$ complexes decrease in intensity. The signals of the CH_3–(O–Al) groups from $Et_2Al(OMe)$ appear at 5.71 ppm in the ^1H NMR spectrum (it is noticeable even at the early stages of the reaction, see Fig. 3B) and at 51.2 ppm in the ^{13}C NMR spectrum.

3.3. Reactions in the mixtures of the catalyst and the cocatalyst

The earlier analysis of the chemical composition of several catalysts of third- and fourth-generation [25,34,35] indicated that a contact between ester-based catalysts and cocatalysts containing $AlEt_3$ and arylalkoxysilanes results in the removal of a large fraction of the esters from the solids and their replacement with alkoxysilanes. Our data provide several spectroscopic proofs of these exchange reactions and identify both the extent and the chemical structure of the leaving products (Sections 3.3.1 and 3.3.2) and the deposition of new compounds on the catalyst surface.

When slurry of the solid catalyst in an aliphatic solvent and the cocatalyst mixture described in the previous section are brought into contact, several chemical interactions take place. Some of the final products of these reactions remain in the solid (they include the active centers of polymerization reactions), other become dissolved. Both these phases, the solid and the solution, were examined separately. Because the cocatalyst mixture has a large excess of $AlEt_3$ with respect to (Cy)(Me)Si(OMe)$_2$ (the molar [Al]:[Si] ratio in the cocatalyst is, typically, 10:1 to 20:1), the most evident of such reactions are those between $AlEt_3$ and different complexes DIBP and PHTHCl on the surface of the solid catalyst, and reactions between $AlEt_3$ and $TiCl_4$. Some of these reactions were studied separately in model systems.

3.3.1. Model systems DIBP–$AlEt_3$

Reactions between DIBP and $AlEt_3$ are similar to the reactions between monoesters of aromatic acids and organoaluminum compounds [2]. They proceed through two distinct stages, the formation of complexes and chemical reactions between the ester groups in the complexes and free $AlEt_3$.

Complexes between organic esters and organoaluminum compounds are well described in the literature [21–25]. DIBP/$AlEt_3$ complexes form very rapidly even at room temperature; they have bright yellow color. Both the ^{1}H NMR spectrum (recorded ~15 min after mixing DIBP and excess of $AlEt_3$ ([$AlEt_3$]:[ester] = 10), and the ^{13}C NMR spectrum (recorded over a period of several hours) showed that all the ester in the mixture is converted into the complexes. The complex formation most strongly affects the α-CH_2 signal of the C(=O)–O–CH_2–$CH(CH_3)_2$ group in the ^{1}H NMR spectrum. This signal in the spectrum of the free ester is a multiplet in the 4.34–4.36 ppm range. The spectrum of the complexes contains three doublets, 3.98–4.01, 4.77–4.79, and 4.83–4.85 ppm. The first two of the doublets have equal intensities and can be tentatively assigned to the 1:1 complex:

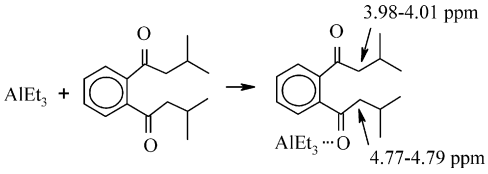

(4)

A doublet of a smaller intensity at 4.83–4.85 ppm probably represents the CH_2 group in a 2:1 complex in which both carbonyl groups are coordinated to Al atoms of $AlEt_3$:

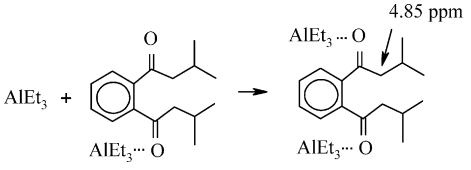

(5)

The formation of these two complexes also produces several changes in the ^{13}C NMR spectrum: the (CH_2) signal is shifted from 71.3 ppm in the spectrum of the free diester to 72.5 ppm, and two groups of (C=O) signals of the complexes replace the 166.7 ppm signal of the free DIBP, one at 173.5 ppm (the 1:1 complex) and another at 176.1 and 177.1 ppm (the 2:1 complex).

Both types of DIBP/$AlEt_3$ complexes formed in reactions (4) and (5) are unstable in the presence of excess $AlEt_3$. Free $AlEt_3$ reduces carbonyl groups of DIBP with the formation of several Al alkoxide species [24]:

$$\text{Complexes } AlEt_3/\text{DIBP} + AlEt_3 \rightarrow Et_2Al\text{–O–}CH_2\text{–}CH(CH_3)_2 + Et_2Al\text{–O–}CEt_2\text{–(Ph)}, \text{ etc.} \quad (6)$$

Reaction (6) accelerates at elevated temperatures (Table 2, experiment 10). It can be easily followed by ^{1}H and ^{13}C NMR: the spectral features of the complexes generated in reactions (4) and (5) gradually disappear and new signals characteristic of diethylaluminum alkoxides from reaction (6) appear at 3.9–4.0 and 5.7 ppm in the ^{1}H NMR spectrum and at 1.03 ppm [(CH_3)–CH_2–Al]; and at 70.8, 71.1, 72.5, 88.3, and 88.7 ppm [C–O–Al)] in the ^{13}C NMR spectrum.

3.3.2. Reactions of catalyst with cocatalyst mixtures, solid products

The interaction between the solid catalyst and $AlEt_3$–(Cy)(Me)Si(OMe)$_2$ mixtures is a complex multi-stage process. Several such reaction products were prepared under the conditions of increasing severity; see Table 1. The effects of the catalyst–cocatalyst reactions on the transmittance IR spectrum of the solid products are shown in Fig. 4. The quantitative estimation of the extent of these reactions (in Table 4) is based on the diffuse reflectance IR spectra.

When the reaction conditions are mild, at [Al]:[Ti] = 30 and 70 °C (Table 1, experiment 2), the combined content of the carbonyl species remaining in the solid product is ~35% of that in the original catalyst. When the reaction between the catalyst and the cocatalyst is carried out under realistic polymerization conditions, at [Al]:[Ti] = 180 and at 80 °C (experiment 4), only ~20% of the initial carbonyl species remain in the solid. On the microscopic level, the catalyst consists of relatively narrow rod-like crystallites built of very small crystals of $MgCl_2$ [16]. This morphologic feature signifies that a fraction of DIBP molecules in the catalyst is buried inside the $MgCl_2$ crystallites and is inaccessible to the cocatalyst. Based on the data on the amounts of DIBP remaining in the solid catalyst after the reactions with the cocatalyst, one can conclude that the surface of the final solid catalyst after the treatment with the cocatalyst is essentially free of any carbonyl species.

The carbonyl complexes of different types have different reactivities in reactions with $AlEt_3$. The IR data (both transmission and reflectance spectra) show the following changes when the solid catalyst is reacted with $AlEt_3$ under conditions of increasing severity:

1. Physisorbed PHTHCl exhaustively reacts with $AlEt_3$ even under the mildest reaction conditions, at [Al]:[Ti] = 24:1 at 20 °C. This compound is not observed in any other solid reaction products

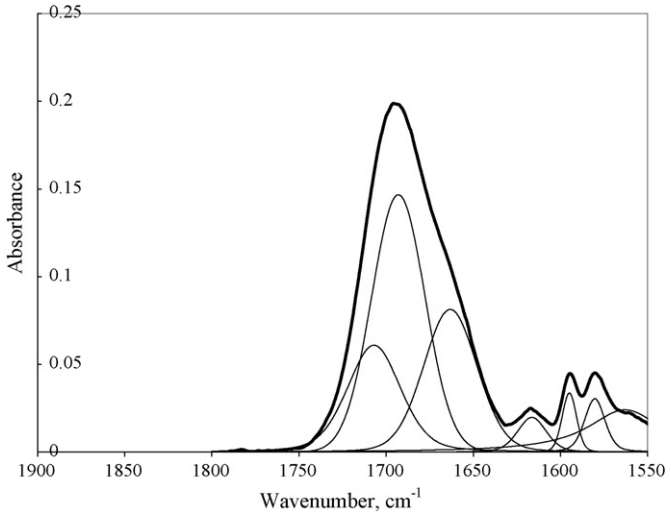

Fig. 4. Transmission IR spectrum [the ν(C=O) range] of reaction products of solid catalyst with $AlEt_3$–(Cy)(Me)Si(OMe)$_2$ cocatalyst mixture at 70 °C. [Al]:[Ti] = 30, [Al]:[Si] = 11 (Table 1, experiment 2).

Table 4
Reactions between $TiCl_4/MgCl_2$/phthalate catalyst and $AlEt_3$ + (Cy)(Me)$Si(OMe)_2$ cocatalysts, amounts of carbonyl complexes remaining in solid products

Complex	Total [C=O] (%)	$MgCl_2$–PhCl (%)	$MgCl_2$–DIBP (%)	$TiCl_4$–DIBP (%)
Initial catalyst	100	30	53	17
Mild reaction conditions, [Al]:[Ti] = 30, 20 °C	~35	~4	~25	~4
Standard reaction conditions, [Al]:[Ti] = 180, 80 °C	~20	~3	~15	~3

of the catalyst and cocatalysts either. This change in the make-up of the solid catalyst could be expected based on the published data on high rates of reactions between acid chlorides and AlR_3 [27].

2. The complex of $MgCl_2$ and PHTHCl also rapidly disappears from the solid; see Table 4.
3. The only two carbonyl-containing species remaining in the catalyst after the treatment with the cocatalyst are the DIBP/$MgCl_2$ complexes and the DIBP/$TiCl_4$ complex.
4. The relative fraction of the $TiCl_4$/DIBP complex (Figs. 1 and 4, the band at ~1670–650 cm^{-1}) in the solid catalyst remains approximately the same in proportion to the $MgCl_2$/DIBP complex: the former complex accounts for 10–15% of all diester species remaining in the reaction products. This conclusion is consistent with the morphological data [16]: Mg and Ti species are distributed uniformly throughout the body of the original catalyst particles.

These data give the following order of reactivity of carbonyl species in the catalyst with $AlEt_3$:

free PHTHCl > PHTHCl/$MgCl_2$ complexes

> DIBP/$MgCl_2$ complexes ≈ DIBP/$TiCl_4$ complexes.

While a large fraction of the ester species is removed from the solid catalyst after its reaction with the $AlEt_3$–(Cy)(Me)$Si(OMe)_2$ cocatalyst mixtures, XPS spectra of these solid products clearly demonstrate that both Al and Si species are deposited on the surface. Even when the reaction between the solid catalyst and the $AlEt_3$–(Cy)(Me)$Si(OMe)_2$ mixture is carried out under very mild conditions, at [Al]:[Si] = 24:1 at 20 °C (Table 1, experiment 1), the surface of the treated catalyst contains significant amounts of Al species [the Al(2p) signal at 75.5 eV] and Si species [the Si(2p) signal at 102.3 eV]. The atomic [Al]:[Ti] ratio on the surface of this mixture is ~6 and the [Si]:[Ti] ratio is ~2.4. The nature of the adsorbed Al and Si species is discussed in Sections 3.3.3 and 3.3.5, respectively.

3.3.3. *Reactions of solid catalyst with cocatalyst mixtures, soluble products*

NMR analysis of soluble products from the reaction between the catalyst and $AlEt_3$–(Cy)(Me)$Si(OMe)_2$ mixtures is complicated by the fact that these solutions are quite dilute. Nevertheless, NMR analysis of the liquids (Table 1, experiments 2, 3 and 6) in comparison with the spectra of model $AlEt_3$–(Cy)(Me)$Si(OMe)_2$ mixtures described in Section 3.2 (Fig. 3) showed important differences between the model systems and the real products of the catalyst/cocatalyst interactions.

When these catalyst/cocatalyst reactions are carried out at high [Al]:[catalyst] ratios, under conditions similar to those in polymerization reactions, either with free $AlEt_3$ (experiment 6 in Table 1) the 10:1 $AlEt_3$–(Cy)(Me)$Si(OMe)_2$ mixture (experiment 3), the solutions, as expected, mostly contain unreacted $AlEt_3$ and very small quantities of aluminum alkoxides produced in reaction (6). ^1H, ^{13}C, and ^{27}Al NMR spectra of these liquids contain the same but barely discernable signals of aluminum alkoxides as those in the spectrum of the heated $AlEt_3$–DIBP mixture (Table 2, experiment 10). The liquid layer in experiment 3 also contains a small quantity of $AlEt_3$/(Cy)(Me)$Si(OMe)_2$ complexes (reactions (4) and (5)).

The catalyst/cocatalyst interaction in experiment 2 in Table 1 was carried out with the $AlEt_3$–(Cy)(Me)$Si(OMe)_2$ mixture at the [Al]:[Ti] ratio of merely 30. NMR analysis of this solution in comparison with spectra of similar model mixtures (Table 2, experiments 8 and 10) was expected to provide information about generation of aluminum alkoxides (products of reaction (6)) in real catalyst systems. Indeed, a relatively low ratio between $AlEt_3$ and the ester groups in this experiment, ~3, and a high temperature, 70 °C, resulted in a significant conversion of $AlEt_3$ in reaction (6): NMR signals of free $AlEt_3$ [signals of CH_2 groups at 0.70–0.8 ppm in the ^1H NMR spectrum, the CH_2–(Al) signal at 0.42 ppm in the ^{13}C NMR spectrum] have disappeared from the solution spectra. However, the expected products of reactions (3) and (6) were not observed in the liquid layer either:

1. The signals of the expected product of reaction (3), $Et_2Al(OMe)$, which are prominent in the NMR spectra of model $AlEt_3$–(Cy)(Me)$Si(OMe)_2$ mixtures (5.71 ppm in ^1H NMR, 51.2 ppm in ^{13}C NMR), are absent from the solution over this catalyst–cocatalyst mixture.
2. Signals of the expected products of reaction (6), Et_2Al–O–CH_2–$CH(CH_3)_2$ and Et_2Al–O–CEt_2–(Ph) species (71–89 ppm in ^{13}C NMR) are not present in the spectrum as well.

Both these observations suggest that most of the three expected diethylaluminum alkoxides, $Et_2Al(OMe)$, Et_2Al–O–CH_2–$CH(CH_3)_2$, and Et_2Al–O–CEt_2–(Ph), are nearly completely adsorbed on the catalyst surface, in agreement with the XPS data for the solid products.

3.3.4. *Reactions of the solid catalyst with cocatalyst mixtures, reduction of Ti species*

The reduction of Ti^{4+} species in supported Ziegler-Natta catalysts upon contact with organoaluminum cocatalysts is described

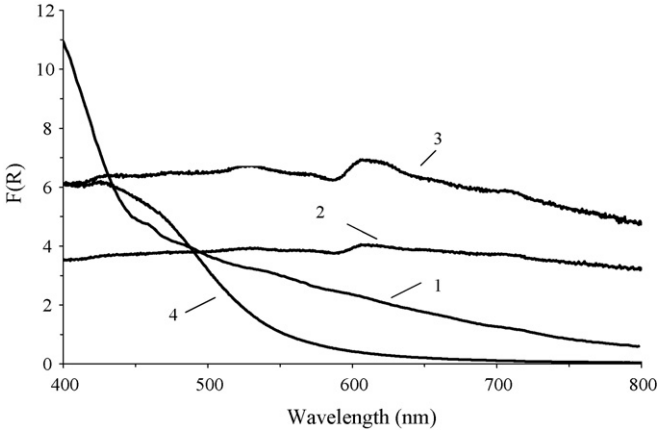

Fig. 5. Diffuse reflectance UV–vis spectra: (1) original solid catalyst, (2) products of catalyst interaction with $AlEt_3$, (3) solid reaction products, (4) solution over reaction products.

in a large number of publications [28–31]. Most of these data were produced by exhaustive hydrolysis of the catalysts and titration of Ti^{IV}, Ti^{III}, and Ti^{II}; they were supported by identification of different Ti^{III} species by ESR. These procedures provide information about all titanium atoms in the catalyst, both the atoms positioned on the surfaces of catalyst particles and those buried inside the $MgCl_2$ matrix. The UV–vis internal reflectance spectroscopy also can be used to examine the Ti reduction reaction. Although this technique is only suitable for a qualitative determination of the valence state of transition metal atoms, it has one advantage for the characterization of Ziegler-Natta catalysts: the UV–vis data mostly reflect the valence of the Ti atoms on the catalyst surface. Fig. 5 compares diffuse reflectance UV–vis spectra of the solid catalyst, the solid phase of the catalyst/cocatalyst reaction products, and the solution over these reaction products, as well as the spectrum of the combined mixture. The original solid catalyst has a featureless spectrum with the absorption gradually increasing from low energy to high-energy wavelengths. Below 450 nm, the absorbance increases due to DIBP coordinated to Ti^{IV}. After addition of $AlEt_3$, this strong short-wave absorption band in the spectrum of the solid significantly decreases in intensity (because DIBP is converted in reaction (6), as described Sections 3.3.1 and 3.3.2) while the absorption increases in the whole visible spectral region. The bands appearing at 524, 608, and 706 nm in the spectrum of the catalyst after addition of $AlEt_3$ reflect the reduction of Ti^{IV}. In general, Ti^{III} complexes have absorption bands in the 550–750 nm range while Ti^{II} complexes absorb at even lower energies, 700–1400 nm [32]. Fig. 5 shows that the dominant reduced Ti species in the catalyst treated with $AlEt_3$ is Ti^{III}. The solution over the $AlEt_3$-treated catalyst has a UV–vis band below 550 nm, which is associated with the complexes of carbonyl-containing compounds with $AlEt_3$ (see reactions (4) and (5)). The absence of reduced Ti species in the solution implies that the Ti species do not leave the solid catalyst after the reaction with $AlEt_3$.

3.3.5. Complexes of (Cy)(Me)Si(OMe)$_2$ with solid catalyst component

As mentioned in Section 3.3.2, XPS spectra of solid products formed in the mixtures of the solid catalyst and the $AlEt_3$–(Cy)(Me)Si(OMe)$_2$ cocatalyst show that the surface of the treated catalyst contains significant amounts of Al and Si species. The NMR data support this observation. The ^{29}Si spectrum of the soluble products in experiment 2 in Table 1 ([Al]:[Si] = 30, [Al]:[Ti] = 30, 70 °C) contains only traces of the signals associated with $AlEt_3$/(Cy)(Me)Si(OMe)$_2$ complexes and the spectrum of the soluble products formed at a much higher [Al]:[Ti] ratio (experiment 3, [Al]:[Ti] = 180 at 80 °C) contains only weak signals of these complexes. Together, these data agree with the XPS results that most of the silane leaves the solution and is adsorbed on the catalyst surface.

The adsorption of (Cy)(Me)Si(OMe)$_2$ and its reaction products with $AlEt_3$ (reaction (3)) on the catalyst surface was further confirmed by IR. The IR spectrum of pure (Cy)(Me)Si(OMe)$_2$ contains a very strong ν[C–O(Si)] band at 1093 cm^{-1}. The high absorption coefficient of this band makes the IR spectroscopic method a convenient tool for detecting alkoxysilanes on the catalyst surface. The IR spectrum of a model mixture of dry $MgCl_2$ and (Cy)(Me)Si(OMe)$_2$ vigorously co-ground in the Nujol medium (Table 2, experiment 11) is practically identical to that of pure (Cy)(Me)Si(OMe)$_2$, i.e., (Cy)(Me)Si(OMe)$_2$ does not form strong, easily observable complexes with $MgCl_2$, in contrast to $MgCl_2$/ester complexes which are easily formed under the same conditions (see Section 3.1.1) This observation agrees with the literature. Although highly dispersed $MgCl_2$ can absorb significant amounts of arylalkoxysilanes in its pores [25], the solid-state ^{13}C NMR study of these mixtures showed that the coordination between RSi(OMe)$_3$ and $MgCl_2$ is quite weak, the silane compounds can be considered as inter-crystalline fluids in the pores of $MgCl_2$ microcrystals [33]. It should be also noticed that any interaction between the silanes and the solid catalysts at the beginning of polymerization reactions does not involve any vigorous mechanical mixing but merely a chemical reaction between the silanes and the catalyst surface.

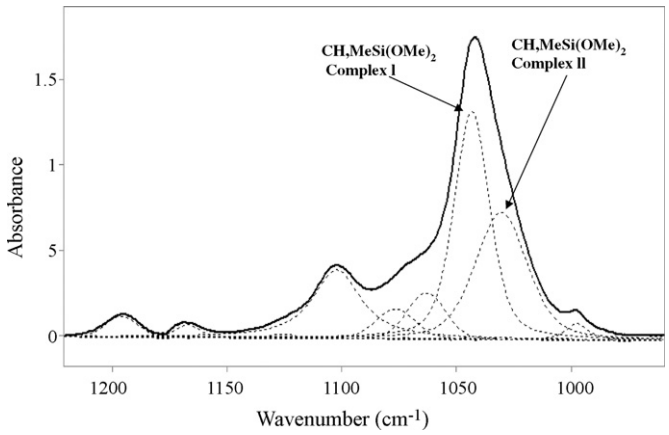

Fig. 6. IR spectrum [ν(C–O) range] of catalyst treated with $AlEt_3$–(Cy)(Me)Si(OMe)$_2$ mixture at 70 °C (Table 1, experiment 2).

When the products of catalyst/cocatalyst interactions are examined by IR in the ν[C–O] range, DIBP molecules coordinated to different inorganic compounds should be taken into account. Neat DIBP has two bands in this region, at 1122 and 1072 cm^{-1}, and a ground mixture of $MgCl_2$ and DIBP (Table 2, experiment 13) contains several overlapping bands at 1160–1140 cm^{-1} and a narrow band at 1078 cm^{-1}. The spectrum of the original solid catalyst contains practically the same pattern: a broad band at ~1155 cm^{-1} (an overlap of four small bands) and a narrow band at 1082 cm^{-1}. All these bands most probably originate from DIBP complexes described in Section 3.1.1.

When a mixture of the catalyst and (Cy)(Me)Si(OMe)$_2$ was reacted under the same conditions (Table 2, experiment 12), the IR spectrum of the mixture, in addition to the DIBP-related bands, contained three other prominent features. The first of them was a medium-intensity band at 1102 cm^{-1}. Its position is close to the band of free (Cy)(Me)Si(OMe)$_2$ (at 1093 cm^{-1}) and its possible origin is a weak coordination complex between (Cy)(Me)Si(OMe)$_2$ and $MgCl_2$, similar to weak complexes of alkoxysilanes and $MgCl_2$ described in the literature [33]. The spectrum of the catalyst–(Cy)(Me)Si(OMe)$_2$ mixture also contained two strong, closely spaced bands at 1042 and 1026 cm^{-1}. These two bands can be tentatively assigned to complexes of (Cy)(Me)Si(OMe)$_2$ with $TiCl_4$-derived species in the catalyst.

Fig. 6 shows the IR spectrum (the 1250–950 cm^{-1} range) of the solid products formed in the reaction between the catalyst and the $AlEt_3$–(Cy)(Me)Si(OMe)$_2$ mixture (experiment 1 in Table 1). This spectrum, as well as IR spectra of other solid products from the catalyst reacted with $AlEt_3$–(Cy)(Me)Si(OMe)$_2$ mixtures (experiments 2 and 3) shows the same two intense bands of the (Cy)(Me)Si(OMe)$_2$/Ti complexes at 1042 and 1026 cm^{-1}, whereas the narrow DIBP-derived band of the catalyst at 1082 cm^{-1} is greatly diminished in intensity. These results confirm the data in Section 3.3.2 (based on ν[C=O] data) that $AlEt_3$ removes a large part of DIBP from the catalyst. The ratio between the two surface (Cy)(Me)Si(OMe)$_2$/Ti complexes changes as the severity of the

reaction between the catalyst and the $AlEt_3$–(Cy)(Me)Si$(OMe)_2$ mixture increases:

Reaction conditions ([Al]:[Ti]; temperature (°C))	2.4; 20	2.8; 70	~19; 80
Complex I (1042 cm^{-1})/complex II (1026 cm^{-1})	4.6	3.6	1.3

These data specify the nature of the transformations in the catalyst make-up known earlier from chemical analysis [25,34,35]: the ester molecules and acid chloride molecules (formed in reaction (2)) are removed from their complexes both with $MgCl_2$ and $TiCl_4$. In parallel, several silane complexes with the catalyst components are generated, the most prominent of which are surface complexes between the silanes and reduced Ti species in the catalysts.

4. Conclusions

The supported Ziegler-Natta catalyst of the fourth-generation designed for propylene polymerization contains several species derived from DIBP, the diester used in its synthesis:

1. Complexes of $MgCl_2$ with DIBP (the dominant products).
2. A complex of $TiCl_4$ with DIBP.
3. Physisorbed PHTHCl (this compound is generated in a reaction between DIBP and $TiCl_4$ during the catalyst synthesis, reaction (2)).
4. Several complexes of $MgCl_2$ with PHTHCl.

These results agree with the literature data [10–14].

When the solid catalyst is contacted with a cocatalyst, a combination of $AlEt_3$ and (Cy)(Me)Si$(OMe)_2$, all these adsorbed carbonyl species vigorously react with $AlEt_3$. The reactions include the reduction of the carbonyl groups of DIBP and the formation of various dialkylaluminum alkoxides. The order of reactivity of the carbonyl species in the reactions with $AlEt_3$ is: physisorbed PHTHCl > PHTHCl/$MgCl_2$ complexes > DIBP/$MgCl_2$ complexes ≈ DIBP/$TiCl_4$ complexes.

These reactions result in complete removal of all PHTHCl species from the catalyst and in significant reduction of the content of the $MgCl_2$/DIBP and $TiCl_4$/DIBP complexes. Taking into account that a fraction of the ester complexes is buried inside $MgCl_2$ crystallites in the solid catalyst and is inaccessible to $AlEt_3$, it is reasonable to assume that practically all carbonyl species are removed from the surface of the catalyst particles upon their treatment with the cocatalyst. The catalyst–cocatalyst reactions also result in the reduction of surface Ti^{IV} species in the solid material, predominantly to Ti^{III} species.

Complexes of (Cy)(Me)Si$(OMe)_2$ with $AlEt_3$ present in the cocatalyst mixture are strongly adsorbed on the surface of the solid catalyst and on the products of its reactions with $AlEt_3$. The most probable coordination site for the silane is reduced Ti species on the surface, including the active centers in olefin polymerization reactions.

References

[1] B.A. Krentsel, Y.V. Kissin, V.I. Kleiner, L.L. Stotskaya, Polymers Copolymers of Higher α-Olefins, Hanser, Munich, 1997.
[2] Y.V. Kissin, Alkene Polymerization Reactions with Transition Metal Catalysts, Elsevier, Amsterdam, 2008.
[3] M. Ferraris, F. Rosati, S. Parodi, E. Giannetti, G. Motroni, E. Albizzati, US Patent 4,399,054 (1983) (to Montedison S.p.A.).
[4] M. Fujita, M. Sakuma, M. Tachikawa, M. Kuzaki, M. Miyazaki, Eur. Patent Appl. 187,035 (1986).
[5] K.E. Mitchel, G.R. Hawley, D.W. Godbehere, US Patent 4,988,655 (1991).
[6] V.M. Frolov, V.I. Kleiner, B.A. Krentsel, R.G. Mardanov, K.A. Munshi, Makromol. Chem. 194 (1993) 2309.
[7] J.J.A. Dusseault, C.C. Hsu, J. Macromol. Sci.: Rev. Macromol. Chem. Phys. C 32 (1993) 103.
[8] M. Kohyama, C. Tagarashi, K. Fukui, Eur. Patent Appl. 172,961 (1986).
[9] L. Luciani, J. Seppälä, B. Lofgren, Prog. Polym. Sci. 13 (1988) 37.
[10] G.G. Arzoumanidis, N.M. Karayanis, Appl. Catal. 76 (1991) 221.
[11] G.G. Arzoumanidis, N.M. Karayanis, Stud. Surf. Sci. Catal. 56 (1990) 147.
[12] C.B. Yang, C.C. Hsu, Y.S. Park, H.F. Shurvell, Eur. Polym. J. 30 (1994) 205.
[13] P. Sobota, J. Utko, T. Lis, J. Organomet. Chem. 393 (1990) 349.
[14] A.G. Potapov, G.D. Bukatov, V.A. Zakharov, J. Mol. Catal. A: Chem. 246 (2006) 248.
[15] B. Mao, A. Yang, Y. Zheng, J. Yang, Z. Li, US Patent 4,861,847 (1989).
[16] M. Chang, X. Liu, P.J. Nelson, G.R. Munzing, T.A. Gegan, Y.V. Kissin, J. Catal. 239 (2006) 347.
[17] C.-P. Cheng, M.D. Spencer, US Patent 6,469,112 (2002).
[18] E. Rytter, S. Kvisle, O. Niriswin, M. Ystenes, H.A. Oya, in: R.P. Quirk (Ed.), Transition Metal Catalyzed Polymerizations. Ziegler-Natta and Metathesis Polymerizations, Cambridge Univ. Press, New York, 1988, p. 292.
[19] M. Ystenes, E. Rytter, Spectrochim. Acta 48A (1992) 543.
[20] M. Ystenes, E. Rytter, Spectrosc. Lett. 20 (1987) 519.
[21] J.C.W. Chien, J.-C. Wu, C.-I. Kuo, J. Polym. Sci. A: Polym. Chem. Ed. 21 (1983) 725.
[22] N. Kashiwa, in: R.P. Quirk (Ed.), Transition Metal Catalyzed Polymerizations: Alkenes and Dienes, Harwood Acad. Publishers, New York, 1983, p. 379.
[23] R. Spitz, J.-L. Lacombe, M.J. Primet, J. Polym. Sci. A: Polym. Chem. Ed. 22 (1984) 2611.
[24] Y.V. Kissin, A.J. Sivak, J. Polym. Sci. A: Polym. Chem. Ed. 22 (1984) 3747.
[25] E. Albizzati, M. Galimberti, U. Giannini, G. Morini, Makromol. Chem.: Macromol. Symp. 48/49 (1991) 223.
[26] E. Iiskola, P. Sormunen, T. Garoff, E. Vahasarja, T.T. Pakkanen, T.A. Pakkanen, in: W. Kaminsky, H. Sinn (Eds.), Transition Metals and Organometallics as Catalysts for Olefin Polymerization, Springer, Berlin, 1988, p. 113.
[27] Y.V. Kissin, J. Catal. 200 (2001) 232.
[28] J.C.W. Chien, in: R.P. Quirk (Ed.), Transition Metal Catalyzed Polymerizations. Ziegler-Natta and Metathesis Polymerizations, Cambridge Univ. Press, New York, 1988, p. 55.
[29] S. Weber, J.C.W. Chien, Y. Hu, in: W. Kaminsky, H. Sinn (Eds.), Transition Metals and Organometallics as Catalysts for Olefin Polymerization, Springer, Berlin, 1988, p. 45.
[30] J.C.W. Chien, T. Nozaki, J. Polym. Sci. A: Polym. Chem. Ed. 29 (1991) 505.
[31] J.C.W. Chien, Y. Hu, J. Polym. Sci. A: Polym. Chem. Ed. 27 (1989) 897.
[32] A.B.P. Lever, Studies in Physical and Theoretical Chemistry, vol. 33, Elsevier, Amsterdam, 1984, p. 399.
[33] T.T. Pakkanen, E. Vahasarja, T.A. Pakkanen, E. Iiskola, P. Sormunen, J. Catal. 121 (1990) 248.
[34] M.C. Sacchi, I. Tritto, C. Shan, R. Mendici, L. Noristi, Macromolecules 24 (1991) 6823.
[35] M.C. Sacchi, F. Forlini, I. Tritto, R. Mendici, G. Zannoni, L. Noristi, Macromolecules 25 (1992) 5914.